Diapycnal mixing and internal waves in the Saint John River Estuary, New Brunswick, Canada with a discussion relative to the Baltic Sea

Nicole C. Delpeche[a], Tarmo Soomere[a] and Madis-Jaak Lilover[b]

[a] Institute of Cybernetics, Tallinn University of Technology, Akadeemia tee 21, 12618 Tallinn, Estonia; nicole.delpeche@gmail.com
[b] Marine Systems Institute, Tallinn University of Technology, Akadeemia tee 21, 12618 Tallinn, Estonia

Abstract. Results of a detailed oceanographic survey in the Saint John River Estuary, New Brunswick, Canada are presented. It is shown that interfacial mixing occurs in this highly stratified basin at discrete locations at a particular phase of the tide leading to a plunging pycnocline at most of these locations. This process is possibly initiated by different kind of internal waves or/and the changing velocity direction on interaction with the irregular bathymetry. Analysis of the flow structure in terms of the critical Richardson number, based on previous studies in the Baltic Sea, shows that these mechanisms and similar phenomena evidently occur at strong density interfaces in the Baltic Sea area where internal waves are less regular but still essentially contribute to interfacial mixing.

Key words: diapycnal mixing, internal waves, stratification, Saint John River Estuary, Baltic Sea.

1. INTRODUCTION

At first glance, the effects of diapycnal mixing in stratified environments on the local ecosystem may not always be obvious. For instance, it plays a vital role in the distribution of phytoplankton, which then has a chain effect of affecting the nutrient supply and thus fisheries habitat. In stratified environments, when phytoplankton is trapped in a well-lighted mixed surface layer, production tends to be enhanced. If this layer is not replenished with nutrients, which are usually at the bottom layer, then the primary production becomes depleted [1]. The same scenario can also occur with respect to polluted waters in either the surface or bottom layers: mixing can either encourage the dilution of the pollution or cause the spread of it. Thus the presence of active diapycnal mixing may cause both negative and positive impacts on the health of the ecosystem. Knowledge on the

conditions, mechanisms, location and timing of the diapycnal processes plays a major role in allowing decision makers to plan and prepare in the interest of the environment.

The general understanding is that a large part of interfacial mixing may be driven by intermittent patches of small scale turbulence that can be caused by internal gravity waves [2–4]. Data on the density and current velocity structure are usually sufficient to identify the main mechanisms that contribute to the mixing processes. As the spatial and temporal resolution of used sensors is often utilized to their limits, the general opinion of experts is that the used methods need further refinements, specifically to account for the complex dynamics associated with the presence of surface and internal waves [5]. Thus to successfully identify and understand the mechanism that may contribute to diapycnal mixing in the field, in principle collection of data on a microstructure level is required.

Many estuarine studies now employ echosounders that visualize the intensity of acoustic backscatter from density interfaces, turbulence and zooplankton. Their advantage is very fine horizontal and vertical resolution. The disadvantage is that the echosounder data are qualitative and should be complemented by other sensors to obtain quantitative data. The echosounder-based techniques have been widely used worldwide. For example, in the Fraser River, West Canada, where Kelvin–Helmholtz (KH) waves were observed [6]; in the Ishikari River, Japan [7], where Holmboe waves [8] (see [9] for discussion of their nature and relations to Kelvin–Helmholtz waves) have been identified and in the Knight Inlet Sill in Western Canada [10] to describe solitonic wave packets.

This paper presents observations in the Saint John River Estuary (SJRE) on interfacial mixing and the generation and dissipation of different modes of internal waves. Prior to these experiments not much was known on the status of the interfacial mixing mechanism and the processes that may be present in the SJRE. Yet, in previous studies [11,12] it was hinted that in the summer months an increase in surface salinity occurred which suggested that interfacial mixing or advection may be taking place. Interestingly, it was found that these mixing events and internal waves were not observed throughout the whole estuary, but at discrete locations at a particular phase of the tide. These results strongly emphasize that the methodology and resolution, employed in field experiments, is vital in capturing the processes.

Although the hydrophysical conditions in the SJRE and the Baltic Sea are fairly different, there is still clear potential of the applicability of the described results for the Baltic Sea. Besides the dominant vertical mixing mechanism (vertical convection during the cold seasons) there are other processes that drive vertical mixing in the Baltics such as mesoscale eddies, coastal upwellings, internal waves, etc. [13]. For this paper we discuss the possibility of the occurrence of relatively high frequency internal waves in the Baltic Sea pycnoclines using a simplified methodology as to that applied for the SJRE.

This paper is organized as follows. The gradient Richardson number, which is often used to quantitatively identify interfacial mixing, is introduced in Section 2.

Section 3 describes the survey site of the Saint John River Estuary. Section 4 presents the observations and Section 5 presents their interpretation in terms of the Richardson number. Finally, in Section 6 we provide discussion of the potential of the use of the phenomena observed in the SJRE for better understanding of the dynamics of the Baltic Sea.

2. THEORY

The dimensionless gradient Richardson number (Ri) is often used to determine if interfacial mixing may occur in stratified environments. This parameter expresses the relative magnitude of the stabilizing forces of the density stratification over the destabilizing influences of the velocity shear:

$$Ri = \frac{N^2}{\overline{s}^2}, \quad N = \sqrt{-\frac{g}{\rho}\frac{\partial \rho}{\partial z}}, \quad \overline{s} = \sqrt{\left(\frac{\partial u}{\partial z}\right)^2 + \left(\frac{\partial v}{\partial z}\right)^2}, \tag{1}$$

where N is the Brunt–Väisälä frequency, $\overline{s}$ is the velocity shear, $g \approx 9.81\,\text{m/s}^2$ is gravitational acceleration, ρ is average density and u and v are current velocity vector components.

Richardson [14] suggests that the critical value at which mixing can occur in stratified environments is $0 < Ri_c < 1$. Later theoretical investigations have placed the critical value in the range $0 < Ri_c < 0.25$, for the fastest growing instability [15,16]. However, for this study $0 < Ri_c < 1$ was used to cover all of the mixing events.

Notice that Ri only indicates that interfacial mixing can take place and does not reflect the particular mechanism behind it. For that reason the linear stability analysis is often employed to identify the source of the shear induced interfacial mixing (i.e., the type of wave that may have initiated the mixing) a linear stability analysis is often employed. Its principle assumption is that a background flow, when perturbed, may develop instabilities. The properties of the background flow are defined by the characteristics of the velocity and density profiles. The two modes of instabilities that may exist in the case of stratified shear flows are that of the KH wave and the Holmboe wave. In general the pycnocline thickness could be either (i) equal or greater or (ii) smaller than the velocity shear thickness (called thick and thin interface, respectively). For thick interface, KH waves are most likely to initiate diapycnal mixing whereas thin interface is favourable for both KH and Holmboe waves.

For simplicity we shall illustrate this method only with the use of the piecewise linear approximation of the profiles which is a convenient way to describe the background flow in stratified environments [17,18]. These approximations are then used to determine the bulk Richardson number

$$J = \frac{gh}{|U_2 - U_1|^2}\frac{\rho_2 - \rho_1}{\rho_2} \tag{2}$$
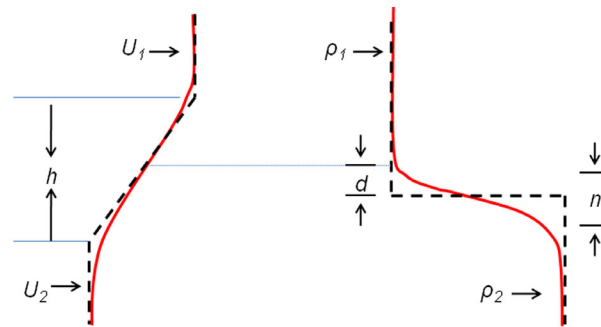
Fig. 1. Piecewise linear approximations of velocity (left) and density (right) profiles; U_1 is the velocity in the upper layer and U_2 in the lower layer, ρ_1 and ρ_2 are the densities in the upper and lower layer, respectively, n is the density interface thickness, h is the shear layer thickness and d is the displacement between the mid-points of the interfaces.

and the asymmetry of the flow $\varepsilon = 2d/h$, where h is the shear layer thickness and d is the displacement of the location of the centre of the pycnocline from that of the shear layer (Fig. 1). Notice that in this case only the velocity in the stream-wise direction (U) is considered and the flow is assumed to be unbounded. Below we apply this approximation to the density and velocity profiles of the SJRE and also to that of the Gotland Deep, Baltic Sea, to identify the possible type of internal waves that may be present.

3. OBSERVATIONS IN THE SAINT JOHN RIVER ESTUARY

The Saint John River originates in the state of Maine, USA, and flows in a southerly direction through New Brunswick where it empties into the Bay of Fundy (Fig. 2). The seaward extent of the estuary is the Reversing Falls and the estuary extends inland to Gagetown which is approximately 60 km from the mouth of the river. There have been several classical [11,12] and recent [19,20] oceanographic studies performed in the Saint John River Estuary.

The Bay of Fundy is famous for having tidal ranges as large as 16 m. At the mouth of the Saint John River the tidal range is approximately 8 m. In the experiment area, which is known as Long Reach (a 4.5 km stretch in the upper section of the Saint John River Estuary), the tidal range is 0.4 m.

The bathymetry and geometry of the Long Reach area are irregular both horizontally and vertically. The water depth varies from 5 to 42 m whilst the width of the study area varies between 300–800 m. Long Reach represents a convenient test area for field studies of semi-diurnal tide-generated phenomena and of the processes that occur more irregularly. The observations for this study were performed in September 2004 when the river discharge was at its lowest for neap tides.

A survey line (Fig. 2) was traversed back and forth during a tidal cycle. Measurements were made of the current velocity, water density and acoustic
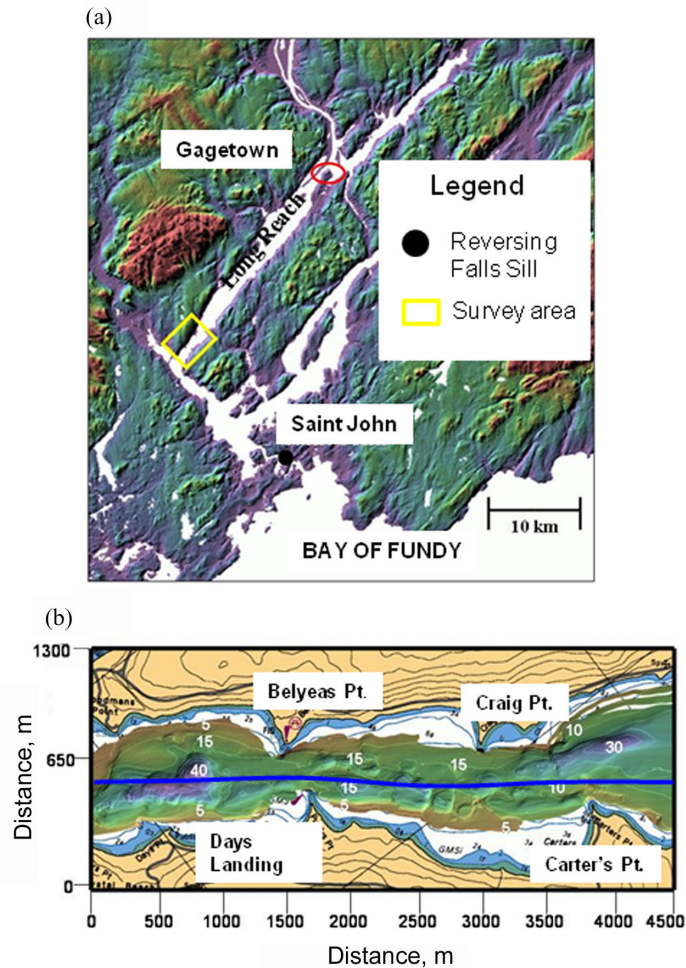
Fig. 2. (a) Map of Saint John River Estuary; (b) bathymetry of the study area in Long Reach. The blue line represents the survey line. On entrance to Long Reach a 42 m deep hole exists, followed by an undulating seabed.

volume backscatter. The sensors used to acquire this data were (i) a 600 kHz Acoustic Doppler Current Profiler (ADCP), which measures current velocity; (ii) a Moving Vessel Profiler (MVP), which is an automated profiler with a CTD (Conductivity Temperature Depth) probe that measures conductivity (C) and temperature (T) of the water column (thereby deriving the salinity (S) from C and T and subsequently density from T and S); and (iii) a 200 kHz echosounder, which produces backscatter from the density interface, zooplankton, turbulence and suspended sediments. The spatial resolutions of these survey sensors differ substantially whereby the echosounder having the best resolution both vertically and horizontally (Table 1).

161

Table 1. Horizontal and vertical resolution of sensors used in survey

| Device	Frequency, kHz	Horizontal resolution, m	Vertical resolution, m
ADCP	600	4	0.5
MVP(CTD)	N/A	400	0.1
Echosounder	200	0.5–1.5	0.07

Due to the difference in the horizontal and vertical resolution of the ADCP and CTD data (Table 1), averaging of the data sets was performed. To perform calculations at the same horizontal and vertical locations, averaging of the CTD data was performed vertically to coincide with that of the ADCP vertical data points whilst the ADCP data was averaged horizontally to conform to the CTD data points. Below we only use the horizontally averaged values of velocity, attributed to the MVP data points.

The echosounder data was processed using software, developed by the Ocean Mapping Group (OMG) from the University of New Brunswick, Canada. The raw echosounder data was first converted to an OMG format allowing convenient production of seismic profiles. From the software the user is capable of defining the horizontal and vertical resolution of each pixel of the plot. As the echosounder has the best resolution in both vertical and horizontal directions (Table 1), this sensor most likely is able to capture from the moving vessel the finestructure processes.

4. OBSERVED FEATURES

The observed data of Long Reach are best interpreted when represented as longitudinal profiles of the density, along velocity and echosounder images. The longitudinal density profiles (Fig. 3) show that the study area of Long Reach is highly stratified for the duration of the entire tidal cycle. The surface layer consists of fresh water with a density of 998 kg/m^3 (salinity of 0.2 psu and temperature of 19 °C) whilst the bottom layer consists of salty water with a density of 1011–1012 kg/m^3 (salinity of 15.0–17.0 psu, temperature of 16 °C). These two layers are separated by a well-defined pycnocline that has an average thickness of 2 m (Fig. 3).

Overall the surface and bottom layer densities in Long Reach remain basically homogeneous for the duration of the tidal cycle. However, two exceptions are observed with respect to the bottom layer. First, the deep hole area (where the depth reaches >40 m, see above) has the densest bottom waters in the whole section (Fig. 4). In this area, current velocities are inconsiderably small throughout the tidal cycle indicating that there is little or no mixing of these waters with water from upstream or downstream. Secondly, at high tide, a decrease in bottom density occurs at a distance about 3700 m from the beginning of the survey line
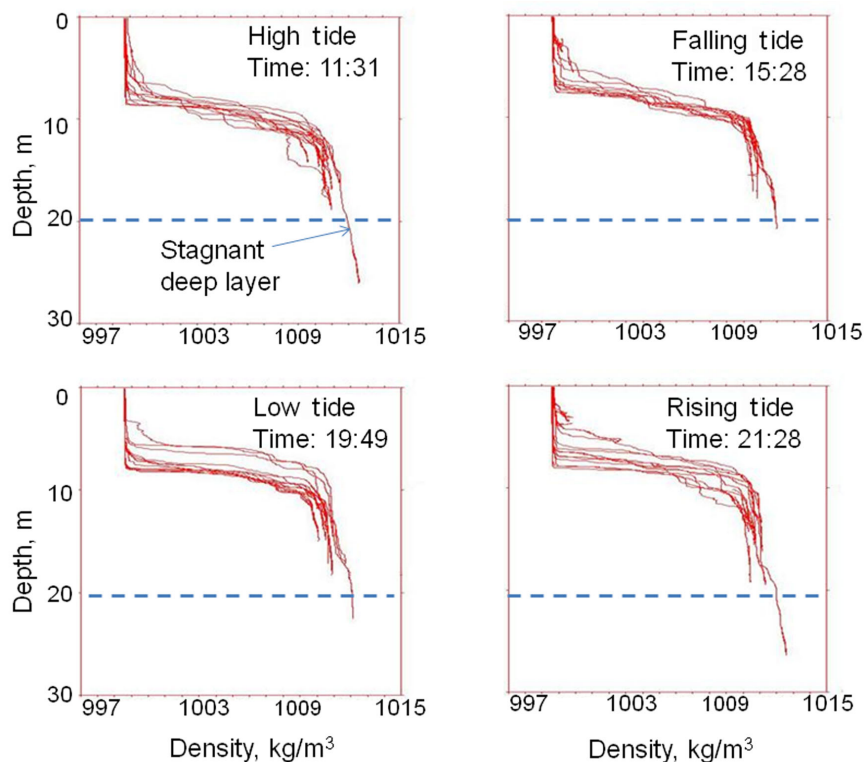
Fig. 3. Density profile plots of all CTD casts at high tide, falling tide, low tide and rising tide.

in the vicinity of Carters Point (Fig. 2b, at the 3700 m marker). This decrease suggests that either strong turbulent mixing or the advection of water is occurring within this area.

At the pycnocline, the echosounder and density profiles showed some interesting features. During falling tide, the echosounder images revealed the presence of solitonic waves identified by their leading waves at the pycnocline (Fig. 5). The first observations were made at 16:08 at the 2500 and 3400 m markers (Fig. 6). Two hours later more sightings of these waves were observed at the 1100, 1700 and 2300 m markers. The distance between the crests of leading waves of these trains (an analogue of wavelength for transient wave trains) varied from approximately 280 to 710 m.

For most of the observations these waves appeared to be stationary. Only one of the waves (at the 2500 m marker) travelled downstream with an approximate speed of 0.2 m/s. The locations where these solitonic waves are observed coincide with the areas where the bathymetry shoals. At the time of observation the flow direction was downstream in both the upper and lower layers.

163
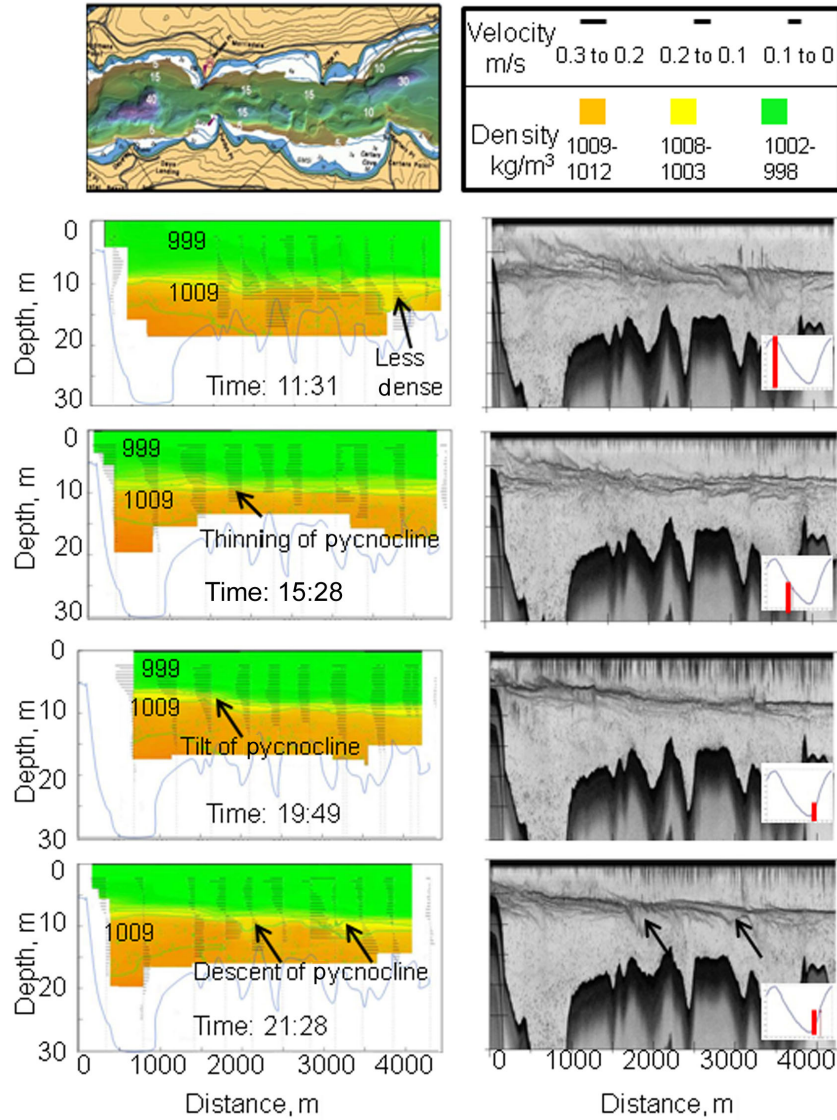
Fig. 4. Longitudinal density and velocity profiles (left) and acoustic volume backscatter images (right) at different phases of the neap tide (inserts; tidal range is about 0.4 m). In the density profiles the arrows to the left represent flow velocities downstream whilst those to the right represent flow upstream. The cross stream flow was found to be negligible and thus omitted.

As the bottom layer flow began to change the direction from downstream to upstream, the solitonic waves experienced dampening or disappearance. The last solitonic wave was observed to disappear between 20:29 and 20:48 (i.e, about 4.5 h from first observation). Interestingly, this time also coincided with the period when maximum velocity shear occurred.

164
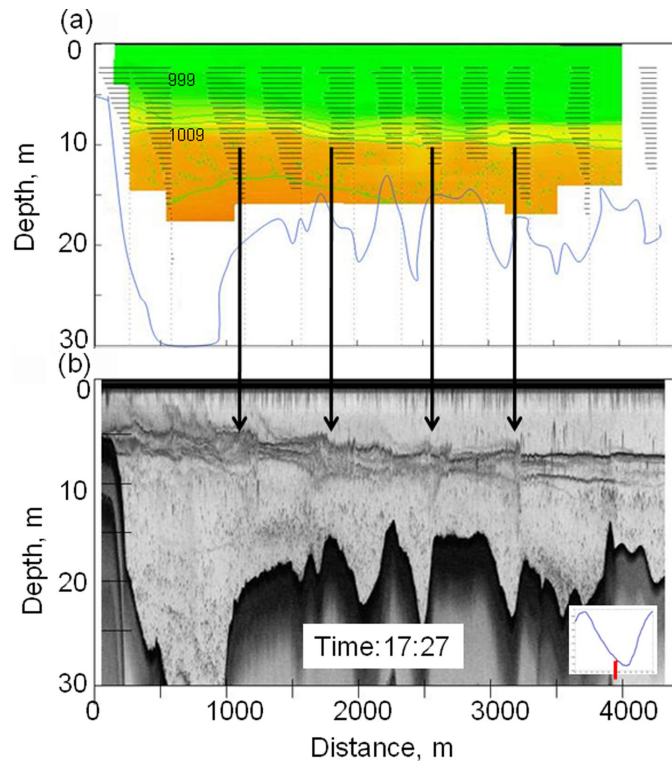
Fig. 5. (a) Longitudinal density and velocity profiles and (b) acoustic backscatter profiles at late falling tide showing the presence of solitonic waves at the pycnocline. The scales and notations are the same as for Fig. 4 except for the velocity scale.

Soon after the disappearance of these solitonic waves (which occurred at the beginning of maximum velocity shear at 20:29) a downward dip of the pycnocline began to occur at distinct locations, where the bathymetry shoals then deepens (Fig. 7).

Following the downward dip of the pycnocline (from 21:28) a thickening of the pycnocline and a decrease in density of the lower portion of the pycnocline takes place (Fig. 7). The downward dips occurred at the edge of the shoals towards the deep areas. Thus the same occurs for the decrease in density and thickening of the pycnocline. It appears to be initiated at the edge of the shoal but continues into the deep areas. Both the echosounder and density profile images were able to capture these discrete events.

As mentioned earlier, a decrease in density continues into high tide and at Carters Pt. a decrease in bottom density was observed. However, at this location, a downward dip of the pycnocline was not observed to occur. Interestingly, however, a downward dip was observed at the 3200 m marker (about 400 m downstream) (Fig. 4).
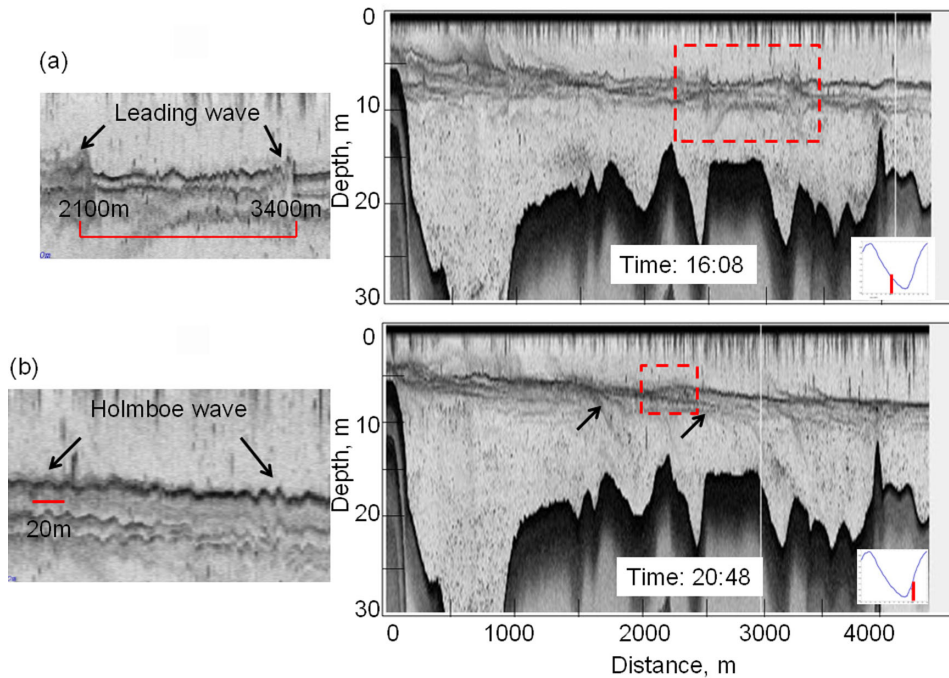
Fig. 6. (a) Echosounder images of solitonic waves on 7 September 2004; (b) echosounder images showing dips in pycnocline (right) and possibly Holmboe waves (left) at 20:48. The left panels represent a zoom of the box in the right panel. Small insertions at right represent phase of the tide as in Fig. 4.
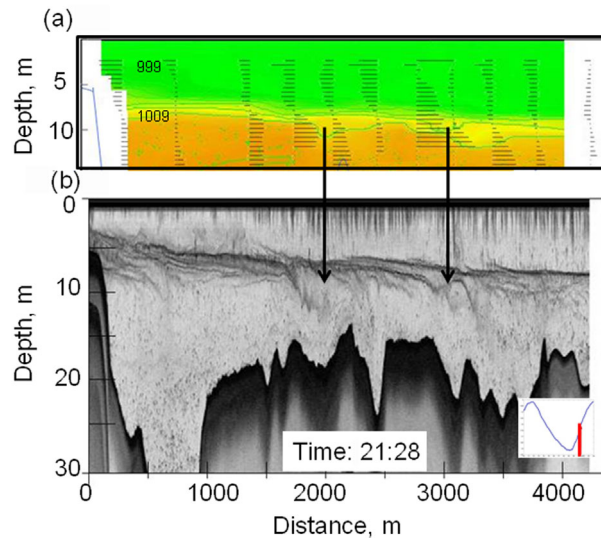

Fig. 7. The downward dip of the pycnocline observed from the density profile (a) and from the acoustic backscatter image (b). Scales and notations are the same as for Fig. 4 except for the velocity scale.

166

5. THE RICHARDSON NUMBER

Using the Richardson number Ri to characterize the type of the flow and the critical Richardson number in the range of $0 < Ri_c < 1$, the results show that interfacial mixing probably started when the downward dip of the pycnocline occurred. This process most likely caused the thickening of the pycnocline and a decrease in density, observed at the base of the pycnocline (Figs. 4a and 7a). Figure 8 illustrates the squared Brunt–Väisälä frequency (N^2) and squared velocity shear $(\bar{s}^2)$, observed for one of the profiles, where interfacial mixing apparently occurred. The area where $\bar{s}^2 > N^2$ (at depths of 6–8 m) is where the interfacial mixing was expected.

At high tide, a decrease in bottom density was observed at Carters Point. However, according to estimates of the Richardson number, mixing was not probable at this location. Instead, the hydrodynamic and hydrophysical conditions were favourable for mixing to occur at the 3200 m marker. Thus, a possible cause for the decrease in bottom density observed at Carters Point (Fig. 5a) is that the mixed water from the vicinity of the 3200 m marker is advected to Carters Point.

To determine if instabilities were possbily present during the mixing process, a linear stability analysis was also performed using a piecewise approximation [17,18]. Figure 9 illustrates an example of the piecewise approximations, performed on one of the velocity and density profiles. The analysis showed that in such an environment non-symmetric Holmboe waves may be present with wavelengths from 8.6 to 10.5 m. The actual presence of Holmboe waves was identified from acoustic backscatter images. They become evident as small amplitude periodic disturbances that were observed throughout the tidal cycle (Fig. 6b). The wavelength, estimated from the observations, varied from 12 to 20 m, which somewhat exceeded the predicted values (Table 2). The uncertainties in the direct readings of wavelengths from echosounder images are 2–3 m.
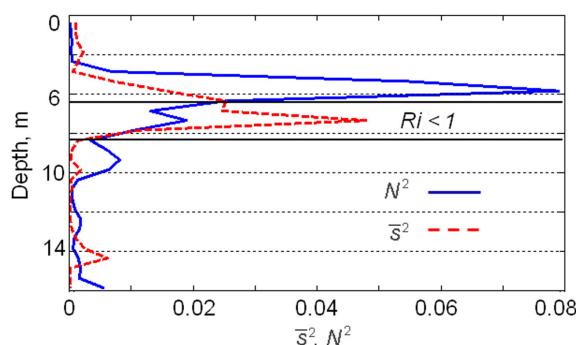
Fig. 8. An example of the estimates of squared Brunt–Väisälä frequency N^2 and squared velocity shear $\bar{s}^2$ for Saint John River Estuary. Interfacial mixing was likely to occur at depths where $Ri < 1$.
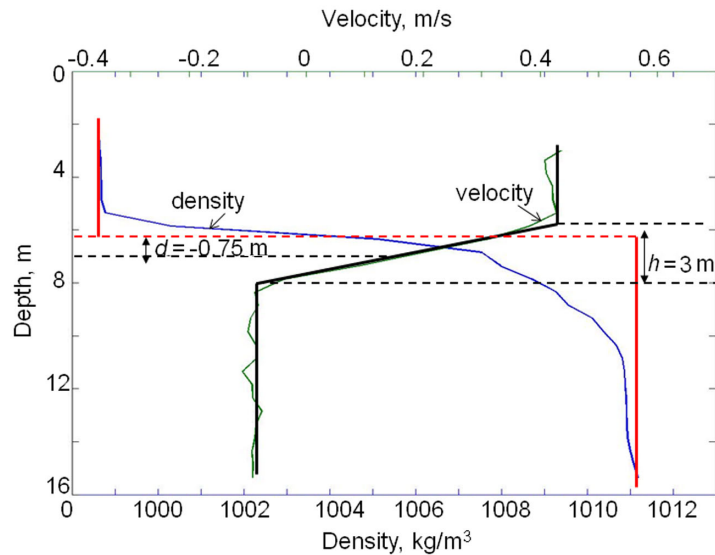
Fig. 9. Density and velocity profile for Long Reach, Saint John River Estuary, for 7 September 2004. The green and blue lines represent velocity and density profiles measured. The red and black lines represent the linear fit, obtained by visual inspection.

Table 2. Results of the linear stability analysis using the piecewise linear approximation, ε refers to the asymmetry of the flow and J is the bulk Richardson number

Time	ε	J	Estimated wavelength, m	Observed wavelength, m
20:41	−0.7	1.43	10.5	12
20:53	−0.5	1.23	8.6	20
20:55	−0.88	0.93	9.7	15
21:57	−0.66	0.996	10.5	14

The uncertainties in the linear stability analysis are mostly connected with the accuracy of visual fits in the piecevise linear approximation of the profiles and apparently are at the same level.

6. DISCUSSION

The observations presented have shown that various processes, potentially leading to enhanced mixing, frequently occur at the pycnocline perturbed by internal waves in stratified environments. These processes can be spatially discrete and become evident as small scale events although their impact on the overall stratification structure and on the functioning of the marine ecosystem can be very vital.

168

The above analysis suggests that in Long Reach interfacial mixing takes place at the time period when maximum velocity shear occurs (at rising tide) at the areas of irregular bathymetry (usually where the bathymetry first shoaled and then the flow met a sharp downward slope). The interfacial mixing was observed to occur at the base of the pycnocline and caused thickening of the pycnocline at certain discrete areas whereas the whole pycnocline did not increase in thickness.

As typical for natural environments, many processes apparently contributed to the observed mixing in the SJRE. The presence of several different types of internal waves suggests that their breaking could play a large role in interfacial mixing. It is also quite possible that a part of the interfacial mixing observed was caused by strongly non-linear effects, created by the motion of solitonic waves and/or the development of Holmboe waves. Another major agent of mixing apparently is the change in the bottom layer velocity from downstream to upstream, as this flow passing over the shoals and then deep areas caused the mixing.

The downward dip of the pycnocline, observed in Long Reach at early rising tide, resembles similar phenomena [3,21] mentioned in the analysis of observations performed by various authors in the New York Bight, Georges Bank, Knight Inlet Sill and in the Strait of Gibraltar [22,23]. The descent of the pycnocline (plunging) was associated either with lee wave down current, caused by the sharp change in bathymetry, or with internal solitary waves, which are the leading edge of an undulatory bore.

6.1. Internal waves and mixing in the Baltic Sea

Comparing the characteristics of the SJRE and the Baltic Sea it is evident that some similarities and differences exist. Historically, both water bodies have been influenced by glacial activity that has created many sills and deep holes, thus creating irregular bathymetry. The Baltic Sea is divided into several basins, based on coastal morphology, sills and topographical formations. The mean depth of the Baltic Sea is around 54 m with the deepest point in the Western Gotland Basin (459 m), which are about ten times larger than the dimensions of the SJRE. Both the basins have a voluminous fresh water supply coming from the rivers and salt water from the ocean. In this sense the Baltic Sea may be considered as a huge estuary [24,25]. The salinity stratification is influenced by the same seasonality pattern and during winter in some parts sea ice is present.

Processes, similar to the ones described above, evidently occur naturally after salt water inflows into the deeps of the Baltic Sea. Strong stratification is created in this basin by the interplay of salt water inflow from the North Sea that flows into the bottom layer and a voluminous supply of fresh water, from the remote eastern and northern parts, that flows into the surface layer [25]. The progression of this saline water into the Baltic Sea and its sub-basins may at times be deferred or advanced depending on the interaction of the bathymetry, wind conditions and sea level differences that maintain a decrease in salinity from the entrance area towards the regions of strong river influence [26,27].

From the Saint John River Estuary examples of interfacial mixing and internal waves were found to be influenced by irregular bathymetry, velocity shear, tides and stratification. Most of these factors are present in the Baltic Sea; however, the time scales and magnitude of these characteristics would vary. The internal dynamics of the Baltic Sea additionally complicates the picture and sometimes three or more clearly defined layers are created at particular locations. Besides a strong permanent halocline at about 60 m depth, a pronounced seasonal thermal stratification takes place at about 20 m depth. These multiple layers affect the distribution and time scale of many vitally important fluxes such as oxygen distribution and transport of nutrients.

A largely open question is how does the mixing at their interfaces occur in the Baltic Sea [27]. Generally, the diapycnal mixing occurs in stratified environment if there is sufficient energy available. The core difference is that the internal waves in the Saint John River Estuary are mainly forced by tides whereas in the Baltic Proper, the main source of energy for internal waves and interfacial mixing comes from the winds [27] and density-driven flows. The wind conditions are dominated by south-westerlies with the strongest winds between October and February and weakest between April and June [25].

Despite the overwhelming dominance of the salinity stratification, diffusive convection has been shown to work in the Baltic halocline enhancing diapycnal mixing [28]. In such conditions, the role of internal waves should be substantial. Considering the internal waves breaking as the major turbulent mixing agent in the deep ocean [29,30], the following parameterization of eddy diffusivity, $K = a_0/N$, where a_0 is a constant, was proposed and successfully used. This success in modelling of the vertical circulation of the Baltic Sea deep water [24] confirms that in the Baltic Sea interior the breaking of the internal waves is one of the major agents of turbulent mixing as well. A recent study of the energy transfer from barotropic to baroclinic wave motion using a two-dimensional shallow water model suggests that about 30% of the energy needed below the halocline for deep water mixing is explained by the breaking of internal waves [31]. Hence, the breaking of internal waves, generated by different mechanisms, could be an important contributor to total diapycnal mixing in the Baltic deep water whereas its role could be even larger at the upper interfaces, where the field of such waves apparently is more intense.

Several studies of diapycnal mixing have been performed in the Baltic Sea such as the DIAMIX survey, performed in 1999–2000 east of Gotland [32] using ADCP and CTD sensors. The results suggest that internal waves and eddies may possibly play a major role in the mixing processes of the Baltic Sea as hypothesized in [26]. There is, however, few publications focusing on the properties of internal waves in the Baltic Sea and on their potential role of the internal dynamics of the basin although their impact has been recognized for decades [33–35]. There is classical evidence that measurements of current velocities and isotherms showed fluctuations of periods 1–30 min in the Kiel Bight and 5–6 h in the Gulf of Finland, Arkona Basin and Darss Sill [25]. These

fluctuations apparently are related to internal waves. Very few studies have employed the echosounder to visualize the processes that are taking place although the role of internal waves in formation of the underwater acoustic field has been mentioned repeatedly [36].

Earlier studies have mostly addressed the overall possibility of the existence of internal waves in the Baltic Sea, but usually have not been focused on establishing which kind of waves (e.g. Kelvin–Helmholtz or Holmboe waves) are present. The marine environment parameters, which determine the wave type, are the Brunt–Väisälä frequency and current velocity vertical shear. It is instructive to consider density profiles through the four seasons to characterize the combination of stratification and velocity shear in the Baltic Proper (Fig. 3.16 of [25]) in terms of the minimum velocity shear $\overline{s}_c = \sqrt{Ri^{-1}N^2}$ that would be required for $Ri < 1$. Table 3 suggests that a velocity shear, greater than about 0.04, is required to initiate interfacial mixing in different layers of the Gotland Deep.

The vertical shear results from a multitude of processes such as wind- and density-driven circulation, mesoscale eddies, slope currents, inertial oscillations, etc. Many *in situ* measurements of current velocity shear were performed by the Estonian Academy of Sciences in the mid-1980s in different basins of the Baltic Sea using a Neil Brawn CTD/ACM profiler with the acoustic current meter system [37]. Relatively high shear and low Richardson number ($Ri \cong 1$) was frequently observed in different water layers (Table 4) [38]. Also persistent layers with $Ri < 1$ were identified in case of presence of near-inertial waves [39,40].

Table 3. Estimates of critical velocity shear (results in $Ri < 1$) and related density parameters extracted from density profiles in ([25], Fig. 3.16)

	Winter	Spring	Summer	Autumn
n, m	40	15	5	15
$\dfrac{\partial \rho}{\partial z}$, kg/m^4	0.26	0.13	0.25	0.15
ρ, kg/m^3	1007	1008	1008	1008
$\overline{s}_c$, s^{-1}	0.05	0.036	0.05	0.038

Table 4. Measured high density gradients (N^2) and velocity shear square ($\overline{s}^2$) in different Baltic Sea sub-basins [37]

Baltic Sea sub-basin	Layer	Physical process	N^2, s^{-2}	$\overline{s}^2$, s^{-2}
Bornholm	Halocline (40–80 m)	Mesoscale eddy	$(20\text{–}25) \times 10^{-4}$	Up to 20×10^{-4}
Eastern part of Gotland Basin	Thermocline and halocline (40–70 m)	Near-slope current	$(2\text{–}20) \times 10^{-4}$	Up to 7×10^{-4}
Entrance area of Gulf of Finland	Below thermocline (25–50 m)	Inertial waves	$(1\text{–}4) \times 10^{-4}$	Up to 4×10^{-4}

The variety of density profiles obtained for the Gotland Deep (Table 3, Fig. 3.16 of [25]) suggest that both thick and thin interfaces (see Section 2) can occur in terms of a piecewise linear approximation depending on the background hydrodynamical processes and therefore both KH and Holmboe waves should contribute to this process. As was shown in the Long Reach example, diapycnal mixing in stratified environments can be initiated by potentially many factors. In the Baltic Sea (where similar conditions are present with respect to bathymetry, stratification and geometry) most of the above-discussed processes may occur as well. While in Long Reach the velocity shear, initiated by tides, played the central role in the diapycnal mixing processes, in the Baltic Sea the mixing processes apparently are initiated by a more random internal wave field, excited by winds, convection, turbulent eddies in the mixed layer and interaction of swells.

A major lesson, learned from the results concerning mixing in Long Reach, is that the mixing processes probably tend to be prevalent where irregular bathymetry, velocity shear and stratification are present simultaneously [26,41]. In the Baltic Sea, various stratification structures are observed that may possibly also evoke similar processes. Another lesson from studies in the Saint John River Estuary is that in order to capture these events, careful consideration should be made to the resolution of the sensors used and the design of the surveys. The use of the echosounder and its resolution capabilities (horizontally and vertically) would allow the capture the role of internal waves in interfacial mixing and to obtain a better understanding of the diapycnal mixing process.

Finally, we note that internal waves with a complex vertical structure and specific properties of three-dimensional propagation may occur under a wide range of continuous stratification. Most of the above observations and theoretical considerations are usually made in the context of 2D waves, propagating along density interface layers. Such layers are relatively weak in the open ocean but frequent and at times fairly strong in estuaries.

ACKNOWLEDGEMENTS

REFERENCES

1. Mann, K. H. and Lazier, J. R. N. *Dynamics of Marine Ecosystems: Biological–Physical Interactions of the Oceans*. Blackwell, UK, 2006.

2. Thorpe, S. Turbulence in stably stratified fluids: A review of laboratory experiments. *Boundary Layer Meteorol.*, 1973, **5**, 95–119.

3. Apel, J. R. *An Atlas of Oceanic Internal Solitary Waves: Oceanic Internal Waves and Solitons*. Global Ocean Associates, prepared for Office of Naval Research, USA, Code 322PO, 2002.

4. Smyth, W. D. and Winters, K. D. Turbulence and mixing in Holmboe waves. *J. Phys. Oceanogr.*, 2003, **33**, 694–711.

5. Burchard, H., Craig, P. D., Gemmrich, J. R., van Haren, H., Mathieu, P.-P., Meier, H. E. M., Smith, W. A. M. N., Prandke, H., Rippeth, T. P., Skyllingstad, E. D., Smyth, W. D., Welsh, D. J. S. and Wijesekera, H. W. Observational and numerical modeling methods for quantifying coastal ocean turbulence and mixing. *Progr. Oceanogr.*, 2008, **76**, 399–442.

6. Geyer, W. R. and Farmer, D. M. Tide-induced variation of the dynamics of a salt wedge estuary. *J. Phys. Oceanogr.*, 1989, **19**, 1060–1072.

7. Yoshida, S., Ohtani, M., Nishida, S. and Linden, P. F. Mixing processes in a highly stratified river. *Physical Processes in Lakes and Oceans: Coastal and Estuarine Studies*, 1998, **54**, 389–400.

8. Holmboe, J. On the behavior of symmetric waves in stratified shear layers. *Geophys. Publ.*, 1962, **24**, 67–113.

9. Caulfield, C. P. and Peltier, W. R. The anatomy of the mixing transition in homogeneous and stratified free shear layers. *J. Fluid Mech.*, 2000, **413**, 1–47.

10. Farmer, D. M. and Smith, J. D. Tidal interaction of stratified flow with a sill in Knight Inlet. *Deep Sea Res.*, 1980, **27A**, 239–254.

11. Trites, R. W. An oceanographic and biological reconaissance of Kennebecasis Bay and the Saint John River Estuary. *J. Fisheries Res. Board Canada*, 1959, **17**, 377–408.

12. Metcalfe, C. C., Dadswell, M. J., Gillis, G. F. and Thomas, M. L. H. *Physical, Chemical and Biological Parameters of the Saint John River Estuary, New Brunswick, Canada*. Department of the Environment Fisheries and Marine Service, Canada. Technical Report No 686, 1976.

13. Reissmann, J. H., Burchard, H., Feistel, R., Hagen, E., Lass, H. U., Mohrholz, V., Nausch, G., Umlauf, L. and Wieczorek, G. Vertical mixing in the Baltic Sea and consequences of eutrophication – a review. *Progr. Oceanogr.*, 2009, **82**, 47–80.

14. Richardson, L. F. The supply of energy from and to atmospheric eddies. *Proc. Roy. Soc. London*, 1920, **A97**(686), 354–373.

15. Miles, J. On the stability of heterogeneous shear flows. *J. Fluid Mech.*, 1961, **10**, 496–508.

16. Miles, J. and Howard, L. N. Note on heterogeneous shear flow. *J. Fluid Mech.*, 1964, **20**, 331–336.

17. Lawrence, G. A., Browand, F. K. and Redekopp, L. G. The stability of a sheared density interface. *Phys. Fluids A*, 1991, **3**, 2360–2370.

18. Haigh, S. P. *Non Symmetric Holmboe waves*. Ph.D. thesis. Department of Mathematics, University of British Columbia, Vancouver, BC, Canada, 1995.

19. Hughes Clarke, J. E. and Haigh, S. P. Observations and interpretation of mixing and exchange over a sill at the mouth of the Saint John River Estuary. In *Proc. 2nd CSCE Speciality Conference on Coastal Estuary and Offshore Engineering*. Toronto, Ontario, Canada, 2005.

20. Delpeche, N. D. *Observations of Advection and Turbulent Interfacial Mixing in the Saint John River Estuary*. M.Sc.E. thesis, University of New Brunswick, Canada, 2006.

21. Apel, J. R., Ostrovsky, L. A., Stepanyants, Y. A. and Lynch, J. F. *Internal Solitons in the Ocean*. Technical Report. Woods Hole Oceanographic Institution, Woods Hole, USA, 2006.

22. Armi, L. and Farmer, D. M. The flow of Mediterranean water through the Straits of Gibraltar. *Progr. Oceanogr.*, 1988, **21**, 1–105.

23. Farmer, D. M. and Armi, L. The generation and trapping of solitary waves over topography. *Science*, 1999, **283**, 188–190.
24. Stigebrandt, A. A model for the exchange of water and salt between the Baltic and the Skagerrak. *J. Phys. Oceanogr.*, 1983, **13**, 411–427.
25. Leppäranta, M. and Myrberg, K. *Physical Oceanography of the Baltic Sea*. Springer Praxis, Chichester, U. K., 2009.
26. Wulff, F., Rahm, L. and Larsson, P. (eds.). *A Systems Analysis of the Baltic Sea*. Springer, Berlin, Heidelberg, 2001.
27. Elken, J., Malkki, P., Alenius, P. and Stipa, T. Large halocline variations in the Northern Baltic Proper and associated meso and basin-scale processes. *Oceanologia*, 2006, **48**(S), 91–117.
28. Kuzmina, N., Rudels, B., Stipa, T. and Zhurbas, V. The structure and driving mechanisms of the Baltic intrusions. *J. Phys. Oceanogr.*, 2005, **35**, 1120–1137.
29. Gargett, A. E. Vertical eddy diffusivity in the ocean interior. *J. Marine Res.*, 1984, **42**, 359–393.
30. Gargett, A. E. and Holloway, G. Dissipation and diffusion by internal wave breaking. *J. Marine Res.*, 1984, **42**, 15–27.
31. Meier, H. E. M., Feistel, R., Piechura, J., Arneborg, L., Burchard, H., Fiekas, V., Golenko, N., Kuzmina, N., Mohrholz, V., Nohr, C., Paka, V. T., Sellschopp, J., Stips, A. and Zhurbas, V. Ventilation of the Baltic Sea deep water: A brief review of present knowledge from observations and models. *Oceanologia*, 2006, **48**(S), 133–164.
32. Stigebrandt, A., Lass, H. U., Liljebladh, B., Alenius, P., Piechura, J., Hietala, R. and Beszczynska, A. DIAMIX – an experimental study of diapycnal deepwater mixing in the virtually tideless Baltic Sea. *Boreal Envir. Res.*, 2002, **7**, 363–369.
33. Lundhansen, L. C. and Skyum, P. Changes in hydrography and suspended particulate matter during a barotropic forced inflow. *Oceanologica Acta*, 1992, **15**, 339–346.
34. Friedrichs, C. T. and Wright, L. D. Resonant internal waves and their role in transport and accumulation of fine sediment in Eckernförde Bay, Baltic Sea. *Cont. Shelf Res.*, 1995, **15**, 1697–1721.
35. Talipova, T. G., Pelinovsky, E. N. and Kõuts, T. Kinematic characteristics of internal wave field in the Gotland deep of the Baltic Sea. *Oceanologiya*, 1998, **38**, 37–46.
36. Vadov, R. A. Long-range sound propagation in the central region of the Baltic Sea. *Acoust. Phys.*, 2001, **47**, 150–159.
37. Lilover, M.-J. *Vertical Fine Structure of Currents in the Baltic Sea*. Ph.D. thesis. Institute of Thermo- and Electrophysics, Tallinn, 1989.
38. Lilover, M.-J. Vertical structure of mesoscale currents in the Baltic Sea. *Ann. Geophys.*, 1992, **10**, Suppl. II, C196.
39. Lilover, M.-J. and Otsmann, M. On the vertical run of inertial waves in the Baltic Sea. In *Proc. 15th Conference of Baltic Oceanographers*. Copenhagen, 1987, 374–387.
40. Lilover, M.-J., Otsmann, M. and Tamsalu, R. Near-inertial waves and shear instability. In *Proc. 16th Conference of Baltic Oceanographers*. Kiel, 1989, 648–652.
41. Polzin, K. L., Toole, J. M., Ledwell, J. R. and Schmitt, R. W. Spatial variation of turbulent mixing in the abyssal ocean. *Science*, 1998, **276**, 93–96.

Siselainete rollist veemasside segunemise protsessis Saint Johni jõe suudmealal New Brunswickis Kanadas ja analoogilisest nähtusest Läänemeres

Nicole C. Delpeche, Tarmo Soomere ja Madis-Jaak Lilover

On esitatud Saint Johni jõe (New Brunswick, Kanada) suudmealal tehtud okeanograafiliste mõõdistuste tulemused ja nende interpretatsioon. On näidatud,

et veemasside vertikaalne segunemine toimub selles tugevalt stratifitseeritud vee-kogus vaid üksikutes kohtades ja kindlates tõusufaasides ning avaldub enamasti püknokliini järsu laskumisena. Segunemise initsiaatoritena toimivad tõenäoliselt mitut liiki siselained ja vahelduva suunaga voolamine suhteliselt kiiresti muutuva sügavusega kohtades. Kihilise voolamise vertikaalse struktuuri analüüsi alusel on näidatud, et vastav mõõduta parameeter – kriitiline Richardsoni arv – on sama-suguste väärtustega mitmetes Läänemere jaoks tüüpilistes situatsioonides, mis-tõttu on tõenäoline, et Saint Johni jõe suudmealal identifitseeritud nähtused (sh siselainete poolt esile kutsutud vertikaalne segunemine) avalduvad sageli Lääne-mere tingimustes.